AMERICAN SOCIETY FOR MICROBIOLOGY | Infection and Immunity

Infiltrated Macrophages Die of Pneumolysin-Mediated Necroptosis following Pneumococcal Myocardial Invasion

Ryan P. Gilley,[a] Norberto González-Juarbe,[a,b] Anukul T. Shenoy,[a,b] Luis F. Reyes,[a,c] Peter H. Dube,[a] Marcos I. Restrepo,[c,d] Carlos J. Orihuela[a,b]

Department of Microbiology and Immunology, The University of Texas Health Science Center at San Antonio, San Antonio, Texas, USA[a]; Department of Microbiology, The University of Alabama at Birmingham, Birmingham, Alabama, USA[b]; Division of Pulmonary Diseases & Critical Care Medicine, The University of Texas Health Science Center at San Antonio, San Antonio, Texas, USA[c]; Division of Pulmonary Diseases & Critical Care Medicine, South Texas Veterans Health Care System, San Antonio, Texas, USA[d]

Streptococcus pneumoniae **(the pneumococcus) is capable of invading the heart. Herein we observed that pneumococcal invasion of the myocardium occurred soon after development of bacteremia and was continuous thereafter. Using immunofluorescence microscopy (IFM), we observed that *S. pneumoniae* replication within the heart preceded visual signs of tissue damage in cardiac tissue sections stained with hematoxylin and eosin. Different *S. pneumoniae* strains caused distinct cardiac pathologies: strain TIGR4, a serotype 4 isolate, caused discrete pneumococcus-filled microscopic lesions (microlesions), whereas strain D39, a serotype 2 isolate, was, in most instances, detectable only using IFM and was associated with foci of cardiomyocyte hydropic degeneration and immune cell infiltration. Both strains efficiently invaded the myocardium, but cardiac damage was entirely dependent on the pore-forming toxin pneumolysin only for D39. Early microlesions caused by TIGR4 and microlesions formed by a TIGR4 pneumolysin-deficient mutant were infiltrated with $CD11b^+$ and Ly6G-positive neutrophils and $CD11b^+$ and F4/80-positive ($F4/80^+$) macrophages. We subsequently demonstrated that macrophages in TIGR4-infected hearts died as a result of pneumolysin-induced necroptosis. The effector of necroptosis, phosphorylated mixed-lineage kinase domain-like protein (MLKL), was detected in $CD11b^+$ and $F4/80^+$ cells associated with microlesions. Likewise, treatment of infected mice and THP-1 macrophages *in vitro* with the receptor-interacting protein 1 kinase (RIP1) inhibitor necrostatin-5 promoted the formation of purulent microlesions and blocked cell death, respectively. We conclude that pneumococci that have invaded the myocardium are an important cause of cardiac damage, pneumolysin contributes to cardiac damage in a bacterial strain-specific manner, and pneumolysin kills infiltrated macrophages via necroptosis, which alters the immune response.**

Community-acquired pneumonia (CAP) is responsible for almost 3.5 million deaths worldwide annually and is one of the most frequent causes of death from an infectious agent around the globe (1–3). Up to one in four adults hospitalized for CAP experience an adverse cardiac event that includes heart failure, arrhythmia, and myocardial infarction (4, 5). These adverse cardiac events predominantly take place during hospitalization, but they also occur at an increased incidence for at least 5 years after hospitalization for CAP, presumably due to lasting cardiac injury (6, 7). *Streptococcus pneumoniae* (the pneumococcus) is the leading cause of CAP, and 19.4% of adults hospitalized for pneumococcal pneumonia in a Veterans Affairs Hospital in Houston, TX, experienced an adverse cardiac event; those that did had a 30-day mortality rate 3.9 times higher than the rate for those with pneumococcal pneumonia alone (8). It remains unclear which pneumococcal virulence mechanisms directly or indirectly impact the heart and how these impacts on the heart lead to the development of an adverse cardiac event (9, 10).

We have recently reported that *S. pneumoniae* forms discrete pneumococcus-filled microscopic lesions (i.e., microlesions) in the heart during invasive pneumococcal disease (IPD) (11). The development of cardiac microlesions was concomitant with aberrant cardiac function in experimentally challenged mice, and former microlesions became focal points of cardiac scarring in animals rescued by antimicrobial treatment. Importantly, pneumococci within cardiac microlesions were shown to produce pneumolysin, a cholesterol-dependent pore-forming toxin (12) which kills cardiomyocytes *in vitro* and has since been shown, along with the bacterial cell wall, to disrupt cardiomyocyte contractility (13, 14). Thus, bacterial entry into the heart and the cardiomyocyte damage caused by pneumolysin are potential explanations for the adverse cardiac events associated with severe CAP.

More recently, Alhamdi and colleagues published a report in which they concluded that circulating pneumolysin in the bloodstream alone was responsible for the cardiac injury that takes place during IPD (14). In contrast to the findings described in our own report (11), Alhamdi et al. failed to detect pneumococci within infected hearts and therefore concluded that myocardial invasion did not occur. One key distinction between the studies was the use of different bacterial strains. We predominantly used TIGR4, a serotype 4 isolate (15), whereas Alhamdi et al. (14) used D39, a

Received 22 January 2016 **Returned for modification** 10 February 2016
Accepted 20 February 2016

Accepted manuscript posted online 29 February 2016

Citation Gilley RP, González-Juarbe N, Shenoy AT, Reyes LF, Dube PH, Restrepo MI, Orihuela CJ. 2016. Infiltrated macrophages die of pneumolysin-mediated necroptosis following pneumococcal myocardial invasion. Infect Immun 84:1457–1469. doi:10.1128/IAI.00007-16.

Editor: A. Camilli

Address correspondence to Carlos J. Orihuela, corihuel@uab.edu.

Supplemental material for this article may be found at http://dx.doi.org/10.1128/IAI.00007-16.

serotype 2 isolate (16). Knowledge of whether or not *S. pneumoniae* invades the heart during IPD has important implications. For example, cardiac scarring at sites of microbial invasion is a potential explanation for the increased incidence of adverse cardiac events that occur during convalescence (6, 11). Also, proof of bacterial invasion would indicate that other cytotoxic compounds produced by *S. pneumoniae*, such as hydrogen peroxide (17), would have direct access to cardiomyocytes. As such, this knowledge directly impacts any potential intervention strategy.

Necroptosis is programmed necrosis. Necroptosis is regulated by receptor-interacting protein 1 kinase (RIP1) and receptor-interacting protein kinase 3 (RIP3) and involves the purposeful disruption of the cell membrane's integrity by the effector mixed-lineage kinase domain-like protein (MLKL) and, thereby, the release of cytoplasmic components, which serve as alarmins. Unlike trauma-induced necrosis, which does not involve cell signaling, necroptosis can be blocked with chemical inhibitors of RIP1 (i.e., necrostatin-5), RIP3 (i.e., GSK'872), and MLKL (i.e., necrosulfonamide). Necroptosis is distinct from intrinsic apoptosis and extrinsic apoptosis, which are caspase dependent and immunologically quiescent (18–20). Pertinent to this study, pore-forming toxins, such as pneumolysin, have been shown to induce alveolar macrophage necroptosis (30). What is more, ischemia-triggered necroptosis is thought to promote adverse cardiac remodeling following an infarct (22).

Here, we provide conclusive evidence that pneumococci that invade the myocardium play an integral role in the cardiac damage observed during IPD, that pneumolysin modifies the host response to pneumococci that invade the myocardium by killing infiltrated macrophages via necroptosis, and that cardiac pathology is strain dependent but not strictly pneumolysin dependent. This study advances our understanding of the host-pathogen interactions that occur in the heart during IPD.

MATERIALS AND METHODS

Ethics statement. All mouse experiments were reviewed and approved by the Institutional Animal Care and Use Committees at The University of Texas Health Science Center at San Antonio (UTHSCSA; protocol number 13032-34-01C). Animal care and experimental protocols adhered to Public Law 89-544 (Animal Welfare Act) and its amendments, Public Health Service guidelines, and the *Guide for the Care and Use of Laboratory Animals* (23).

Bacterial strains. *S. pneumoniae* serotype 4 strain TIGR4 (15) and serotype 2 strain D39 (16) have been sequenced. Isogenic mutants deficient in *ply* and *pspA* were created by insertion of an erythromycin resistance cassette, *ermB*, using allelic exchange, as previously described, and grown in medium supplemented with 1 μg/ml of erythromycin (24, 25). Pneumococci were grown on blood agar plates or in Todd-Hewitt broth containing 0.5% yeast extract at 37°C in 5% CO_2. For infections, cultures were grown to an optical density at 620 nm of 0.5 (mid-log phase) and serially diluted in sterile phosphate-buffered saline (PBS).

Mouse infections. All mice used in the study were 6-week-old female BALB/c mice unless stated otherwise. The mice were challenged by intraperitoneal (i.p.) injection of 10^3 CFU of *S. pneumoniae* suspended in 100 μl sterile PBS using a 27-gauge needle. Intratracheally challenged mice were anesthetized and inoculated by forced aspiration of 10^5 CFU in 100 μl PBS (21). The mice were euthanized at a predetermined time point or if they were deemed moribund. Euthanasia was performed by CO_2 asphyxiation using compressed gas; death was confirmed by the presence of pneumothorax during the collection of hearts. Where indicated, mice received 10 μg necrostatin-5 (catalog number N0164; Sigma, St. Louis, MO) dissolved in dimethyl sulfoxide (DMSO) and diluted with PBS or an equivalent amount of DMSO in PBS to a total of 100 μl by i.p. injection every 6 h and sacrificed at 24 h postinfection (hpi).

Assessment of bacterial burden in blood and troponin in serum. The bacterial burden in the blood of infected mice was determined by serial dilution and plating on blood agar plates and extrapolation from colony counts following overnight incubation. Peripheral blood was collected from anesthetized mice by use of a retro-orbital bleed prior to euthanasia. Clotted blood was then centrifuged at 16,000 × *g* for 10 min, and the collected serum was stored in single-use 100-μl aliquots at −80°C. The serum levels of cardiac troponin-I in mice infected as described above were measured by enzyme-linked immunosorbent assay (ELISA) (Life Diagnostics, West Chester, PA).

Tissue staining. Hearts collected from the mice were placed in cassettes for embedment in paraffin or processing of frozen tissue using the optimal cutting temperature compound OCT (Tissue-Tek). Paraffin-embedded sections were sliced to a thickness of 4 μm and stained with hematoxylin and eosin (H&E); frozen sections were sliced to a thickness of 7 μm and used for immunofluorescence microscopy (IFM). Before staining, frozen sections were fixed with 10% neutral buffered formalin for 10 min, washed twice for 5 min each time with sterile PBS, permeabilized using 0.2% Triton X-100 in PBS for 15 min, and then washed twice for 5 min each time with sterile PBS. The sections were then blocked with PBS containing 5% serum from the species which produced the secondary antibody and 3% bovine serum albumin for 1 h at room temperature. The primary antibodies used in this study included the following: serotype 4 and serotype 2 capsular polysaccharide (CPS) antibodies (catalog numbers 16747 and 16725, respectively; Staten's Serum Institut, Copenhagen, Denmark); anti-Ply (catalog number 71811), CD11b (catalog number 133357), CD3 (catalog number 5690), and phosphorylated MLKL (p-MLKL; catalog number 196436) (all from Abcam, Cambridge, United Kingdom); CD11b (catalog number 550282), Ly6G (catalog number 551459), and CD19 (catalog number 553784) (all from BD Pharmingen); anti-F4/80 (catalog number 25830), anti-arginase I, and anti-arginase II (all from Santa Cruz, Dallas, TX); and anti-RIP3 (catalog number 45842; Novus Biologicals, Littleton, CO). Primary antibodies were diluted 1:1,000 in blocking solution and incubated with tissue sections overnight at 4°C. Following incubation with primary antibody, the samples were washed twice for 30 min each time with 0.2% Triton X-100 in PBS at room temperature and once with PBS for 30 min at room temperature. The sections were then incubated with the respective secondary antibody in blocking solution for 1 h at room temperature: goat anti-rabbit immunoglobulin conjugated with fluorescein isothiocyanate, goat anti-mouse immunoglobulin conjugated with rhodamine, or goat anti-rat immunoglobulin conjugated with Alexa Fluor 647 (all from Jackson ImmunoResearch, West Grove, PA) or donkey anti-rabbit immunoglobulin conjugated with rhodamine (EMD Millipore, Temecula, CA). The sections were then washed twice for 30 min each time with PBS. A single drop of DAPI (4′,6-diamidino-2-phenylindole; Molecular Probes) was placed on the section and allowed to sit for 1 min before being removed; the sections were then washed with PBS. FluorSave (Calbiochem, San Diego, CA) was then added, and the sections were covered with a slide cover.

Microscopy and analysis. H&E-stained images were captured using a Zeiss AxioXam MRm Rev3 and/or MRc camera attached to a Zeiss AxioImager Z1 epifluorescence microscope (Carl Zeiss, Thornwood, NY). Immunofluorescent images were taken at the UTHSCSA microscopy core using a Zeiss LSM 710 confocal microscope with an EC Plan-Neofluar objective (40× oil immersion lens; numerical aperture, 1.3). Transmission electron microscopy images were obtained at the UTHSCSA electron microscopy core using a JEOL JEM1230 transmission electron microscope (Peabody, MA). IFM images of lesions were taken as z-stacks and compressed with the average intensity per slice using ImageJ software. For size and area analyses, lesions were imaged at a magnification of ×20 with a Zeiss AxioImager Z1 epifluorescence microscope and measured using ImageJ software.

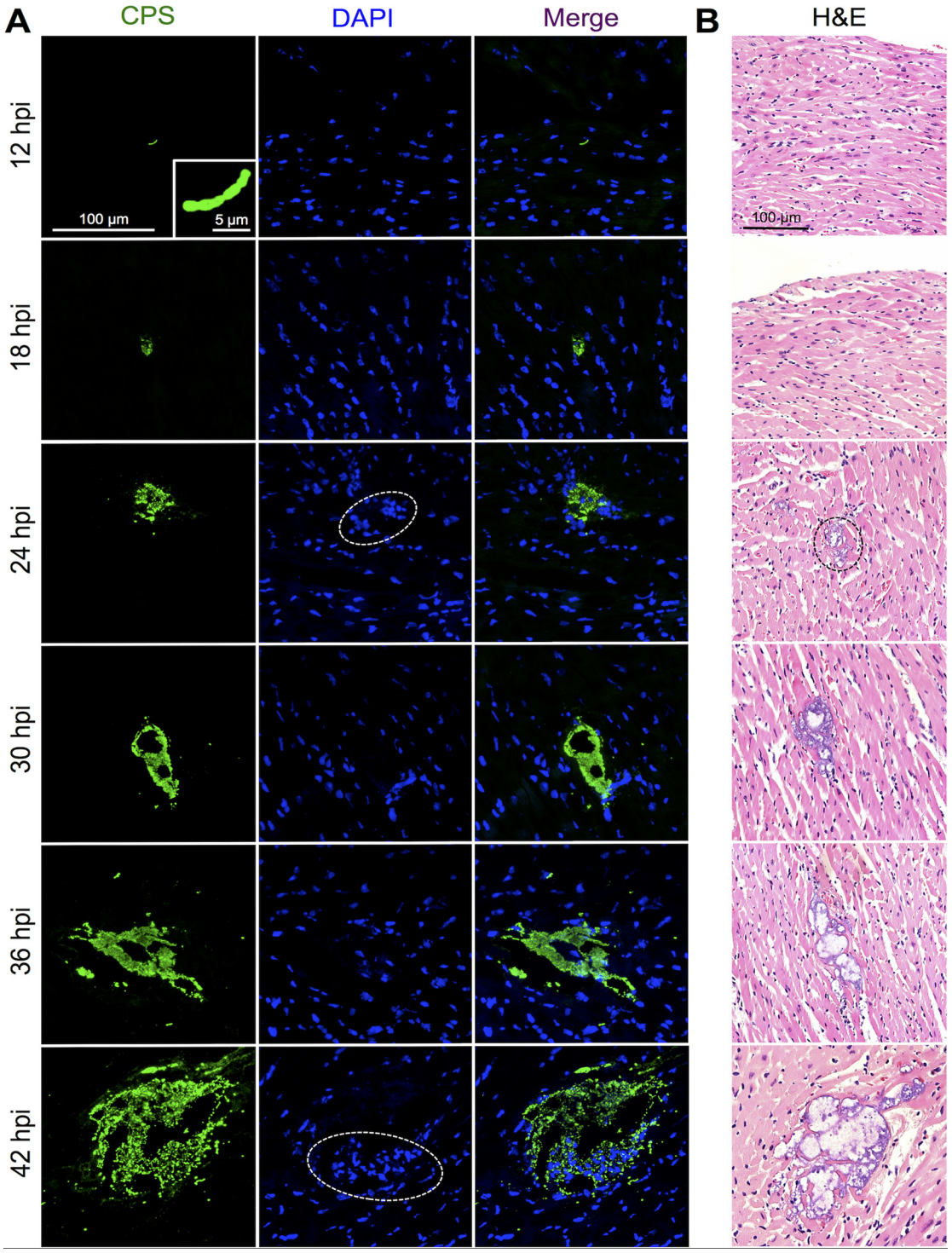

FIG 1 *S. pneumoniae* invasion and replication within the myocardium. Representative high-magnification images of cardiac sections from mice infected with *S. pneumoniae* strain TIGR4 are shown. A minimum of 5 hearts were examined at each time point. (A) IFM of frozen sections stained with serotype 4 CPS antiserum. Dashed ovals, areas where nucleated cells stained with DAPI could be detected at the periphery of microlesions. Magnification, ×40 with a zoom factor of 1.0 and ×40 with a zoom factor 3.0 (inset, 12 hpi). (B) H&E-stained paraffin sections showing representative cardiac microlesions. Dashed oval, first sign of a cardiac microlesion beginning at 24 hpi. Magnification, ×200.

ELISAs. Hearts were perfused with PBS, cut into fourths, washed twice with 1 ml sterile PBS, and homogenized in a protease (catalog number P2714; Sigma) and phosphatase (catalog number 78428; Thermo Scientific, Rockford, IL) inhibitor cocktail diluted in distilled water. Homogenates were centrifuged at 300 × *g* for 10 min to remove the tissue debris; the supernatant was then removed with a pipette and centrifuged at 1,000 × *g* for 5 min to remove the remaining debris. The supernatant homogenate was then frozen in single-use 100-μl aliquots at −80°C.

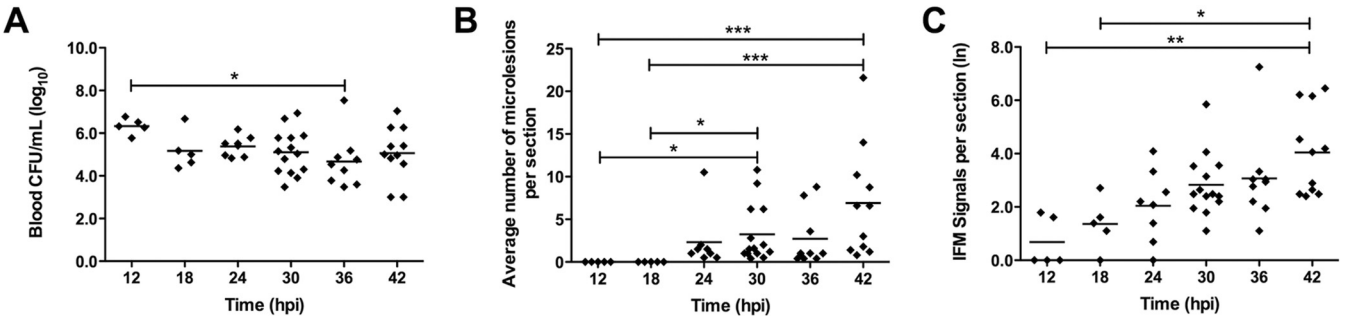

FIG 2 Myocardial invasion is continuous during pneumococcal bacteremia. (A) Bacterial titers in the blood of individual infected mice (diamonds) at the time of euthanasia. (B) Average number of discrete microlesions per heart section detected at each time point on H&E-stained slides viewed at a magnification ×20. The results are averages for 5 nonadjacent sections per heart. (C) Enumeration (natural log) of pneumococcal replication points within heart sections determined by IFM. Black horizontal bars, average value for the cohort. *, $P \leq 0.05$; **, $P \leq 0.01$; ***, $P \leq 0.001$.

Heart homogenates were assayed for interleukin-1β (IL-1β), tumor necrosis factor alpha (TNF-α), and IL-6 (all from BD Biosciences, San Diego, CA); keratinocyte-derived chemokine (KC), macrophage inflammatory protein 2 (MIP-2), and vascular endothelial growth factor (VEGF) (all from R&D Systems, Minneapolis, MN); and granulocyte-macrophage colony-stimulating factor (BioLegend, San Diego, CA) according to the manufacturers' specifications.

Statistical analyses. For multiple-group analyses, we used a nonparametric analysis of variance (ANOVA; the Kruskal-Wallis test) with Dunn's *post hoc* analysis; grouped analyses were performed using a two-way ANOVA. For nonparametric data sets, we used a Mann-Whitney rank sum test. These statistical analyses were performed using Prism (version 5) software (GraphPad Software, La Jolla, CA). Chi-square values were calculated using the Social Science Statistics website.

RESULTS

Pneumococci invade and replicate within the heart, causing strain-dependent pathology. In mice challenged with TIGR4, a serotype 4 isolate, individual diplococci and short chains could be detected within the myocardium as early as 12 hpi (Fig. 1A). Detection was performed using IFM with specific antibody against type 4 capsular polysaccharide (CPS) (see Fig. S1A in the supplemental material). At this time point, mice showed no overt signs of infection yet had bacterial titers in the blood that reached 10^6 CFU/ml (Fig. 2A). By 18 hpi, small clusters of pneumococci could be detected within cardiac sections (Fig. 1A), suggesting that the pneumococci that had invaded the myocardium had begun to replicate. At 18 hpi, the bacterial titers in the blood had diminished to 10^5 CFU/ml and remained relatively constant thereafter (Fig. 2A). Defined microlesions in H&E-stained heart sections, as first described by our group, could be observed only beginning at 24 hpi. In all, discrete microlesions of pneumococci within the heart increased in number and size through 42 hpi (Fig. 1 and 2B; Table 1). Importantly, the number of individual/small clusters of pneumococci ($\leq$100 μm^2) that could be detected only by IFM also increased with time, and individual/small clusters were the predominant assemblage of pneumococci present within the heart at all time points (Fig. 2C; Table 1). This suggests that cardiac invasion from the bloodstream was continuous. Furthermore, 23 to 60% of the intermediately sized microlesions (i.e., those ranging from 101 to 100,000 μm^2) caused by TIGR4 were found to be associated with a focus of nucleated cells at their periphery (Fig. 1A; Table 1). These were not detected in our initial report on cardiac microlesions. Foci of nucleated cells were absent in areas of the myocardium where individual pneumococci or very small clusters ($\leq$100 μm^2) were detected, nor were they associated with the largest microlesions ($\geq$100,001 μm^2) (Table 1).

Finally, we also confirmed that sustained bacteremia was necessary for TIGR4 cardiac microlesion development. Mice challenged with a mutant lacking pneumococcal surface protein A (PspA), which inhibits complement deposition (26, 27), never developed bacteremia and had only transient signs of cardiac invasion (Table 1; see also Fig. S1B in the supplemental material).

Whereas TIGR4 readily formed defined cardiac microlesions, D39, the serotype 2 strain used by Alhamdi et al. (14), did not; only 4 microlesions were detected in all H&E-stained cardiac sections from 8 mice examined at 24 hpi ($\geq$5 sections per mouse; Fig. 3A). However, hearts from D39-infected mice showed considerable damage and had multiple focal points of cardiomyocytes undergoing hydropic degeneration with leukocyte infiltration (Fig. 3B). Although no pneumococci could be seen within these foci in H&E-stained sections, D39 was readily detected at the same site when serial tissue sections were stained for type 2 capsular polysaccharide (Fig. 3B). IFM also revealed considerable numbers of individual D39 pneumococci scattered throughout the myocardium (Fig. 3C). Thus, both TIGR4 and D39 were capable of myocardial invasion. We conclude that invasion of the myocardium by pneumococci requires sustained bacteremia and occurs in a continuous fashion during infection, replication within the heart precedes visual microlesion formation in H&E-stained slides, and different strains of *S. pneumoniae* cause distinct cardiac pathologies.

The pneumolysin contribution to cardiac damage is strain dependent. Given the differences in pathology between TIGR4- and D39-infected hearts, we examined the contribution of pneumolysin to the tissue damage caused by these strains. At 42 hpi, mice infected with either TIGR4 or TIGR4 Δ*ply* had elevated levels of cardiac troponin-I, a marker of cardiac damage, in their serum compared to the levels in the serum of mock-infected mice (Fig. 4A). No significant differences in troponin-I levels between mice infected with the wild-type strain and mice infected with the mutant strain were observed at 18 and 42 hpi, and the bacterial burdens in mice infected with these strains were equivalent (Fig. 4B). In contrast, cardiac damage in D39-infected mice seemed to be exquisitely pneumolysin dependent (Fig. 4C). Of note, D39-infected mice had a mean bacterial burden of $>10^9$ CFU/ml blood and were deemed to be moribund at 24 hpi (Fig. 4D), hence the absence of data for troponin-I levels in D39-infected mice at 42

TABLE 1 *S. pneumoniae* requires pneumolysin to clear lesions of immune cells

Strain	hpi	No. of mice	Total avg no. of signals/ section	≤100 μm²			101–1,000 μm²			1,001–10,000 μm²			10,001–100,000 μm²			≥100,001 μm²		
				Avg no. of signals/ section[a]	% of total lesions	% of lesions with immune cells[b]	Avg no. of signals/ section	% of total lesions	% of lesions with immune cells	Avg no. of signals/ section	% of total lesions	% of lesions with immune cells	Avg no. of signals/ section	% of total lesions	% of lesions with immune cells	Avg no. of signals/ section	% of total lesions	% of lesions with immune cells
TIGR4	12	5	2.8	2.8	100	0	0	0	NA[c]	0	0	NA	0	0	NA	0	0	NA
	18	5	5.6	4.4	78.6	0	0.8	14.3	0	0.4	0	50.0	0	0	NA	0	0	NA
	24	8	15.6	11.4	72.8	0	1.6	10.4	23.1	2.5	16.0	60.0	0.1	0.8	0	0	0	NA
	30	14	41.6	37.8	90.7	0	0.4	0.9	40.0	2.9	7.0	51.2	0.6	1.4	25.0	0	0	NA
	36	10	153.5	147.0	95.8	0	2.8	1.8	28.6	3.0	2.0	46.7	0.4	0.3	12.5	0.3	0.2	0
	42	11	174.4	166.0	95.2	0	0.2	0.1	0	3.9	2.2	44.2	4.2	2.4	21.7	0.1	0.1	0
TIGR4 Δ*ply*	18	5	17.6	16.0	90.9	0	0.8	4.5	25.0	0.8	4.5	50.0	0	0	NA	0	0	NA
	30	6	24.0	22.3	93.1	0	0.2	0.7	100	1.5	6.3	**88.9**[d]	0	0	NA	0	0	NA
	42	6	124.0	118.7	95.7	0	0.2	0.1	100	2.8	2.3	**94.1**	1.8	1.5	**100**	0.5	3.9	**100**
TIGR4 Δ*pspA*	18	6	3.0	3.0	100	0	0	0	NA	0	0	NA	0	0	NA	0	0	NA
	30	6	4.3	4.3	100	0	0	0	NA	0	0	NA	0	0	NA	0	0	NA

[a] The average number of signals per section was determined by averaging the total number of CPS signals per group at each time point.

[b] Immune cell infiltration was determined by the presence of DAPI-positive nucleated cells within the boundaries of the microlesion.

[c] NA, not applicable; percentage could not be generated.

[d] Bold data indicate statistical significance compared with the results for wild-type strain TIGR4 at the same time point and at the same size, as calculated by the chi-square test.

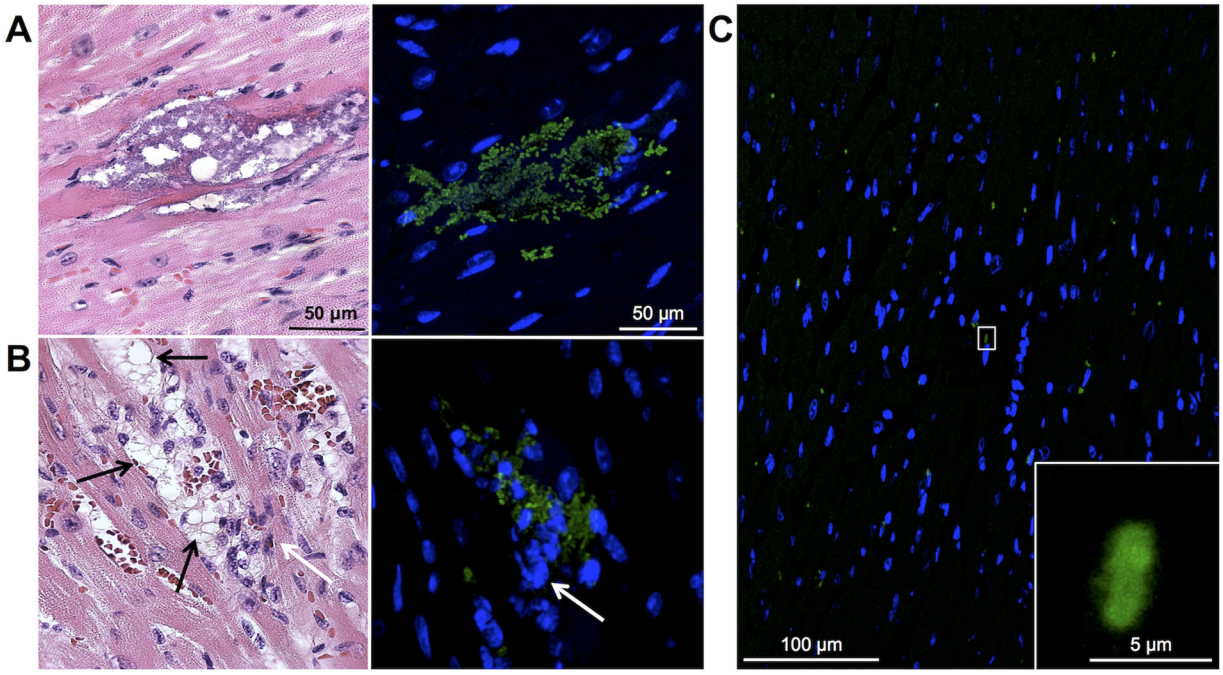

FIG 3 D39 invades the myocardium. High-magnification H&E-stained images (left) and IFM images (right) of a representative discrete cardiac microlesion (A) and immune cell-infiltrated foci (B) in cardiac sections from 10- to 12-week-old mice infected with D39 obtained at 24 hpi. Black arrows, areas of hydropic degeneration; white arrows, infiltrated immune cells. IFM was performed using antiserum against serotype 2 capsular polysaccharide. Images are of the same cardiac microlesion, and serial sections from paraffin-embedded tissue were stained. Magnifications, ×400 (H&E-stained sections) and ×40 with a zoom factor of 1.5 (IFM images). (C) Low-magnification image of an IFM-stained section from a D39-infected mouse showing multiple positive *S. pneumoniae* signals. (Inset) Higher-magnification view of the boxed section. Magnifications, ×40 with a zoom factor of 0.6 and ×40 with a zoom factor of 4.0 (inset).

hpi, yet D39 Δ*ply*-infected mice had sustained bacteremia at a level of ~10^6 CFU/ml blood (Fig. 4D), a level comparable to that in mice infected with TIGR4. Collectively, these results show that D39 requires pneumolysin for cardiac damage, yet the role of pneumolysin remains unclear for TIGR4.

Pneumolysin mediates immune cell clearance within cardiac microlesions. Strikingly, TIGR4 microlesions that were associated with nucleated cells stained weakly for pneumolysin, whereas those devoid of nucleated cells had detectable levels of the toxin when tissue sections were tested by IFM (Fig. 5A). Quantitative analysis of the mean fluorescence intensity confirmed that pneumolysin levels were lower in microlesions associated with foci of nucleated cells than in microlesions not associated with foci of nucleated cells (Fig. 5B). Subsequently, tissue sections from mice challenged with TIGR4 Δ*ply* were examined microscopically. Almost all microlesions (i.e., those of >100 μm^2) formed by TIGR4 Δ*ply* beyond 18 hpi were filled with nucleated cells (Fig. 5C and D; Table 1). As indicated above, at 42 hpi the levels of serum troponin-I in mice challenged with TIGR4 Δ*ply* were also increased and were not statistically significantly different from those in mice challenged with TIGR4 (Fig. 4A), indicating that cardiac damage was incurred despite the recruitment of these cells.

To identify the cell type(s) being recruited to the heart and possibly cleared by pneumolysin, we performed IFM on heart sections containing early TIGR4 microlesions and those from TIGR4 Δ*ply*-infected mice. $CD11b^+$ cells that were Ly6G positive ($Ly6G^+$) were detected throughout the lesion, confirming the presence of neutrophils. Additionally, we observed $CD11b^+$ and $F4/80^+$ cells predominantly at the periphery of microlesions, indicating the presence of macrophages (Fig. 6) (28). We also tested for the presence of enzymatic markers indicative of myeloid suppressor cells, arginase I and arginase II (29), but detected neither. Together these results indicate that cells in purulent microlesions collected early from TIGR4- and TIGR4 Δ*ply*-infected mice were effector macrophages and neutrophils.

Infiltrated macrophages die as a result of necroptosis. Recent publications by us (30) and Kitur et al. (31) indicate that pore-forming toxins trigger alveolar macrophage necroptosis and this results in their depletion from the bacterium-infected airway. Given these results, we hypothesized that the absence of immune cells within the larger established cardiac microlesions may be due in part to pneumolysin-induced necroptosis. Along such lines, we detected the active forms of RIP3 and MLKL, which are a necroptosis activator and effector, respectively (32–34), on the periphery of early immune cell-associated microlesions formed by TIGR4 (Fig. 7A). These were absent in microlesions formed by TIGR4 Δ*ply* (Fig. 7B). These positive signals overlapped with those for $CD11b^+$ myeloid cells (Fig. 7A). To quantitate this, we counted 49 lesions in heart sections obtained from 10 TIGR4-infected mice at between 30 and 42 hpi and found that 74% (36/49) had positive signals for p-MLKL and RIP3 kinase, whereas only 7% (2/28) of lesions in heart sections from mice challenged with TIGR4 Δ*ply* showed positive signals ($P < 0.01$, chi-square analysis). Importantly, early lesions formed by TIGR4 also showed the colocalization of p-MLKL with the macrophage marker F4/80 (Fig. 7C). This was not observed for $Ly6G^+$ cells (data not shown).

Further implicating necroptosis as a key event, mice treated with a necroptosis inhibitor every 6 h following challenge with

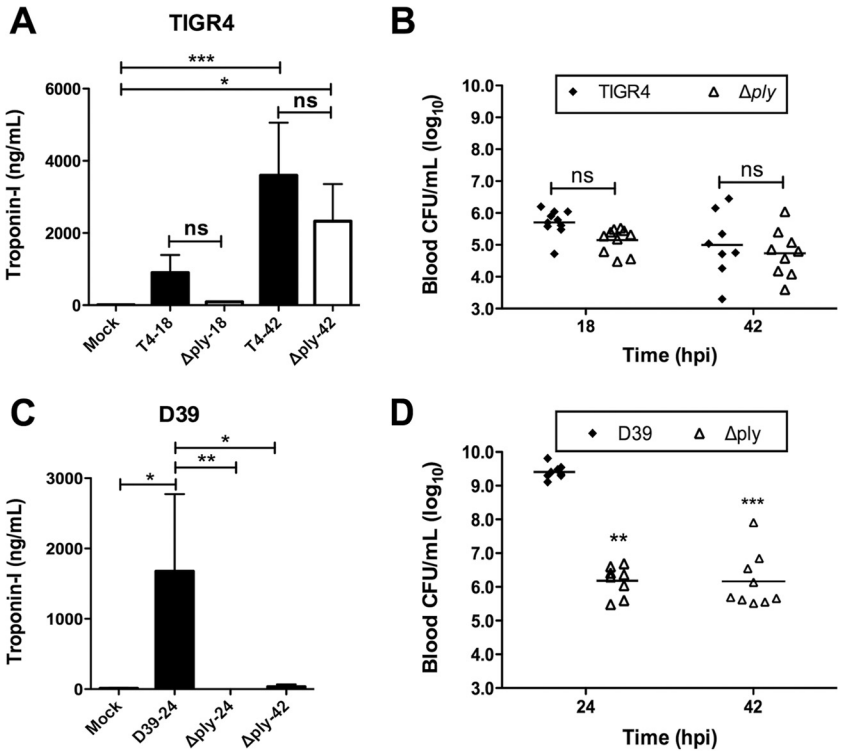

FIG 4 Cardiac damage is incurred following myocardial invasion, and pneumolysin is required in a strain-dependent manner. Cardiac troponin-I was detected in the serum of mice infected with TIGR4 or TIGR4 Δ*ply* (A) and D39 or D39 Δ*ply* (C). The suffixes 18, 24, and 42 on the *x* axis refer to 18, 24, and 42 hpi, respectively. (B and D) Bacterial titers in the blood of mice challenged with TIGR4 and TIGR4 Δ*ply* (B) and D39 and D39 Δ*ply* (D) at the time of sacrifice; for panel D, statistical significance was determined by comparison to the values for D39-infected mice at 24 hpi. Black horizontal bars, average values for the cohort. Asterisks denote statistically significant differences (*, $P \leq 0.05$; **, $P \leq 0.01$; ***, $P \leq 0.001$; ns, not significant).

TIGR4 had normal numbers of cardiac microlesions (see Fig. S2A in the supplemental material); however, the majority of these either had become fully purulent or had immune cells located at their periphery (Fig. 7D; see also Fig. S2B in the supplemental material). We further tested this *in vitro* by exposing human THP-1 macrophages either to wild-type TIGR4 (Fig. 7E) or to recombinant pneumolysin (Fig. 7F). Macrophages pretreated with RIP1, RIP3, or MLKL inhibitors were protected against killing, while those pretreated with the pan-caspase inhibitor carbobenzoxy-valyl-alanyl-aspartyl-(*O*-methyl)-fluoromethyl ketone (Z-VAD FMK) were not. These data support our *in vivo* findings suggesting that infiltrated macrophages die by necroptosis and that this impacts the accumulation of immune cells within the microlesion.

Pneumolysin elicits a cytokine and chemokine response from the heart. Finally, we performed ELISA on homogenates of heart tissue from wild-type TIGR4- and TIGR4 Δ*ply*-challenged mice (Fig. 8). At 42 hpi, we observed increased levels of IL-6 and the chemokine KC but not MIP-2 in hearts from TIGR4-infected mice. In contrast, we observed a weak trend toward increased levels of IL-1β and TNF-α in hearts from mice infected with TIGR4 Δ*ply*. These findings indicate that pneumococci that invade the myocardium elicit an immune response that is modulated by pneumolysin. What is more, the lack of immune cell infiltration in mature TIGR4 microlesions is not due to an inability of cardiomyocytes to produce chemokines.

DISCUSSION

Adverse cardiac events during and after CAP are the result of multiple converging events that occur within the vasculature and heart. Activation of both the coagulation cascade and immune cells in blood vessels contributes to the instability or rupture of atherosclerotic lesions in the coronary arteries, which can lead to myocardial infarction (4, 35). Unintended effects of antimicrobials and poor oxygenation status at a time of increased myocardial demand have been shown to contribute to cardiac complications (36, 37). Ligation of cardiomyocyte Toll-like receptors (TLRs) with pathogen-associated molecular patterns (PAMPs) or damage-associated molecular patterns (DAMPs) in the circulation results in NF-κB-dependent decreases in contractility (10, 38). Along such lines, proinflammatory cytokines in the blood, such as TNF-α, which are produced in response to infection, have also been shown to be cardiosuppressive (40). When these events occur during pneumonia, they can exacerbate preexisting cardiac conditions or lead to new heart failure, arrhythmia, or infarct. The likelihood of death during pneumonia is substantially greater for patients in whom this occurs than for patients with pneumonia alone.

Only recently has evidence emerged showing that bacteria can enter and directly damage the heart during severe pneumonia and subsequent bacteremia. This concept is most advanced for *S. pneumoniae*, where it has been shown that ligation of the platelet-activating factor receptor on cardiomyocytes by cell wall phosphorylcholine has cardiac-suppressive effects (13). Moreover, our initial

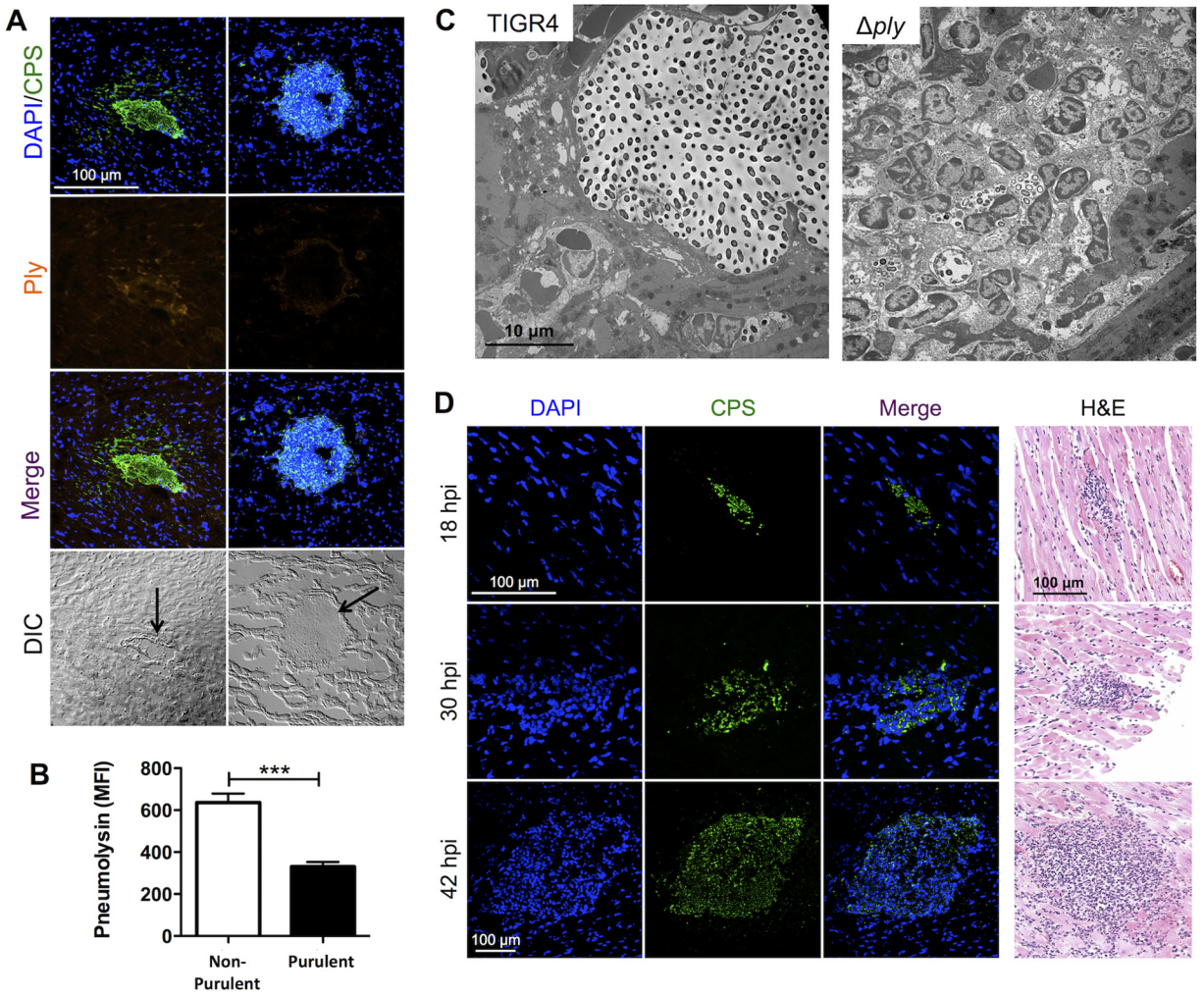

FIG 5 Nucleated cell infiltrates in TIGR4 microlesions are associated with the absence of pneumolysin. (A) IFM images of cardiac sections from TIGR4-challenged mice stained with DAPI and probed with antisera for CPS and pneumolysin (Ply). The majority of TIGR4 microlesions were nonpurulent (left), with pneumolysin being detectable at the lesion site. In some instances, the lesions had a high number of nucleated cells, as detected by staining with DAPI, with significantly lower levels of pneumolysin (right). DIC, differential interference contrast. Magnification, ×40 with a zoom factor of 1.0. (B) Mean fluorescence intensity (MFI) of the pneumolysin detected in nonpurulent versus purulent cardiac microlesions from TIGR4-infected mice measured using ImageJ software. Data are for 11 to 15 lesions from 3 to 4 mice in similar cohorts. ***, $P \leq 0.001$. (C) Transmission electron microscopy of TIGR4- and TIGR4 Δ*ply*-infected mouse hearts showing immune cells located at the periphery and distributed throughout the entirety of the microlesion, respectively. Magnifications, ×6,000. (D) IFM and H&E-stained images of cardiac sections from mice infected with TIGR4 Δ*ply* showing the presence of nucleated cells within the lesion. Magnifications, ×40 with a zoom factor of 1.0 at 18 and 30 hpi and ×20 with a zoom factor of 1.0 at 42 hpi (IFM images) and ×200 (H&E-stained images).

report (11), along with the work of Alhamdi et al. (14), showed that pneumolysin is capable of killing cardiomyocytes. Alhamdi et al. also elegantly showed that sublethal concentrations of pneumolysin impaired contractility due to uncontrolled calcium influx through pneumolysin-formed membrane pores (14). However, the findings as to whether *S. pneumoniae* invades the myocardium described in the work of Alhamdi et al. (14) and those described in our own original report (11) were disparate. In this study, we demonstrate that cardiac invasion by the diverse strains tested, including strain D39, used by Alhamdi et al. (14), does occur, thereby suggesting that other pneumococci are also capable of cardiac invasion.

We attribute the discrepancy between our findings and those of Alhamdi et al. (14) to be principally due to the increased sensitivity of IFM in regard to the detection of pneumococci and the strain-specific differences in virulence and pathology for TIGR4 and D39. As shown herein, D39 rarely formed the discrete microlesions first described by our group when we used TIGR4. Instead, it caused foci of cardiac damage and immune cell infiltration, where bacteria were not readily visible in H&E-stained sections. Which pathology, that caused by TIGR4 or that caused by D39, in mice is most representative of the condition in humans remains unknown and requires further investigation. It is also important to consider that humans are more susceptible to pneumolysin than mice (41). If the pneumolysin-dependent pathology caused by D39 is most representative of the condition in humans, then the obscuring nature of immune cells located in areas of cardiomyocyte hydropic degeneration helps to explain why the discovery of invading pneumococci in human myocardial samples did not occur until recently.

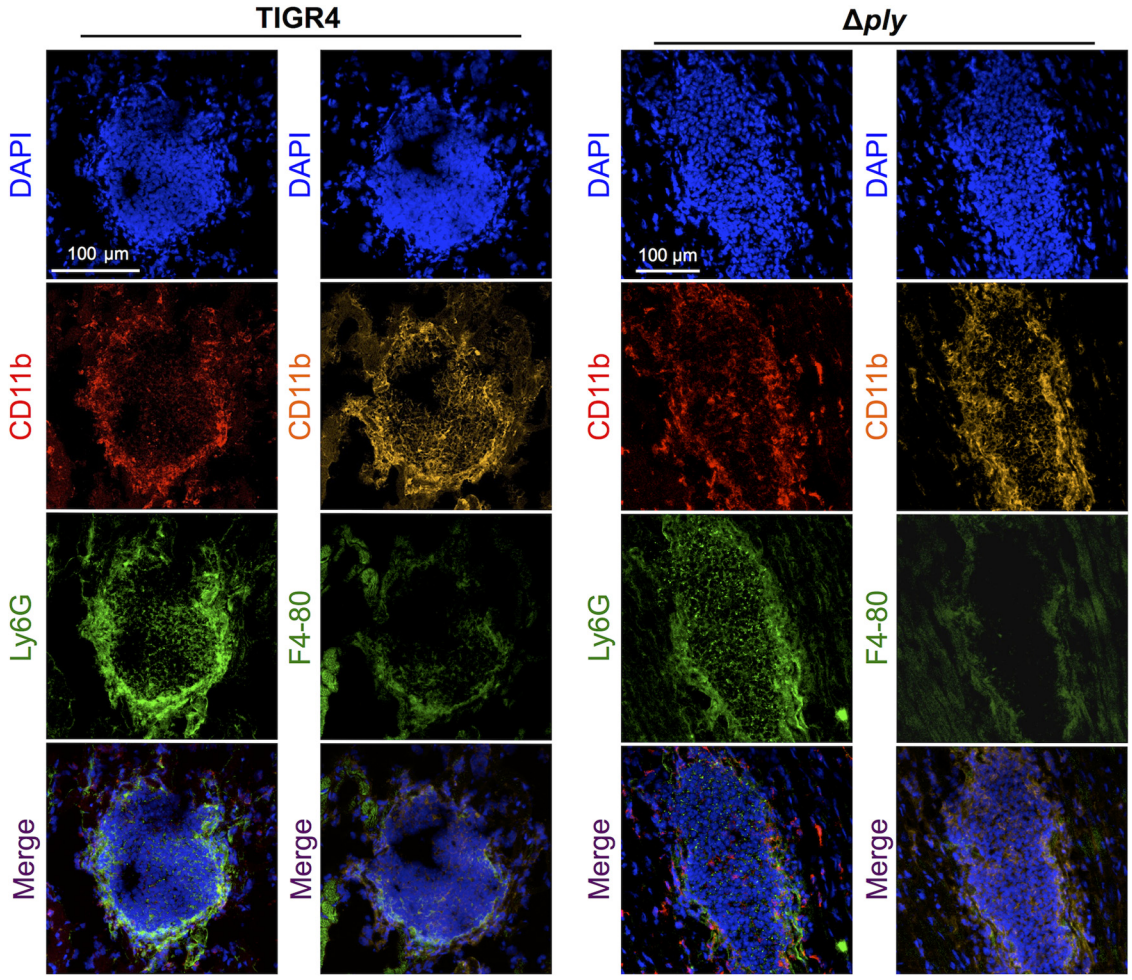

FIG 6 Cardiac microlesions infiltrated macrophages and neutrophils. Representative high-magnification images of cardiac sections from mice infected with TIGR4 or TIGR4 Δ*ply* are shown. Sections were stained with DAPI and the myeloid marker CD11b for the detection of nuclei and costained with either the neutrophil marker Ly6G or the macrophage marker F4/80. Magnification, ×40 with a zoom factor of 0.8 (TIGR4) and a zoom factor of 0.6 (TIGR4 Δ*ply*).

Our results do not exclude the possibility that circulating pneumolysin in the bloodstream is a meaningful cause of cardiac damage, as suggested by Alhamdi et al. (14); however, the presence of D39 in areas of the heart where cardiac damage was most evident does suggest that pneumococci that invade the myocardium are themselves a principle mediator of cardiac damage. Highlighting this point as well as the considerable differences between the tested strains, a TIGR4 mutant lacking pneumolysin was able to cause cardiac damage, as determined by measurement of the serum levels of troponin-I and pathological examination of hearts. This demonstrates that, depending on the invading strain, factors other than pneumolysin may contribute to cardiac damage. Some obvious candidates would be the hydrogen peroxide produced by the pneumococcal pyruvate oxidase (17), as well as secreted enzymes that target host molecules, such as metalloproteases (42). Strain-specific differences in the presence of such virulence determinants or in their level of expression within the heart are also a reasonable explanation for the observed differences in pathology. Along such lines, we speculate that the reason that smaller lesions contain immune cells is that pneumolysin must accumulate and this occurs as pneumococci replicate and the microlesion grows.

We did not observe neutrophils that underwent pneumolysin-induced necroptosis. These cells may have susceptibility to cholesterol-dependent cytolysins different from macrophages (43). Regardless, the reason for their eventual clearance remains unknown. It is possible that other factors produced by the pneumococcus kill these cells or, alternatively, that neutrophils are self-depleted following netosis (44). Death by necroptosis is highly proinflammatory due to the release of alarmins from cells (45), yet during TIGR4 infection, necroptosis of macrophages and the cytokines and chemokines produced within the infected heart were not sufficient to trigger a continuous wave of immune cell infiltration into microlesions. We speculate that this is because TIGR4-infected animals experience severe systemic disease and the chemokine gradients arising from other organs may be stronger than those arising from the heart. It is of note that the production of pneumolysin by pneumococci that invaded the myocardium potentiated only the KC and IL-6 responses within infected hearts. This suggests that other ligands produced by the pneumococcus, such as the TLR1/2 ligand cell lipoteichoic acid (46), or the direct cardiac injury caused by pneumococci that invade the myocardium is sufficient to instigate an equivalent response consisting

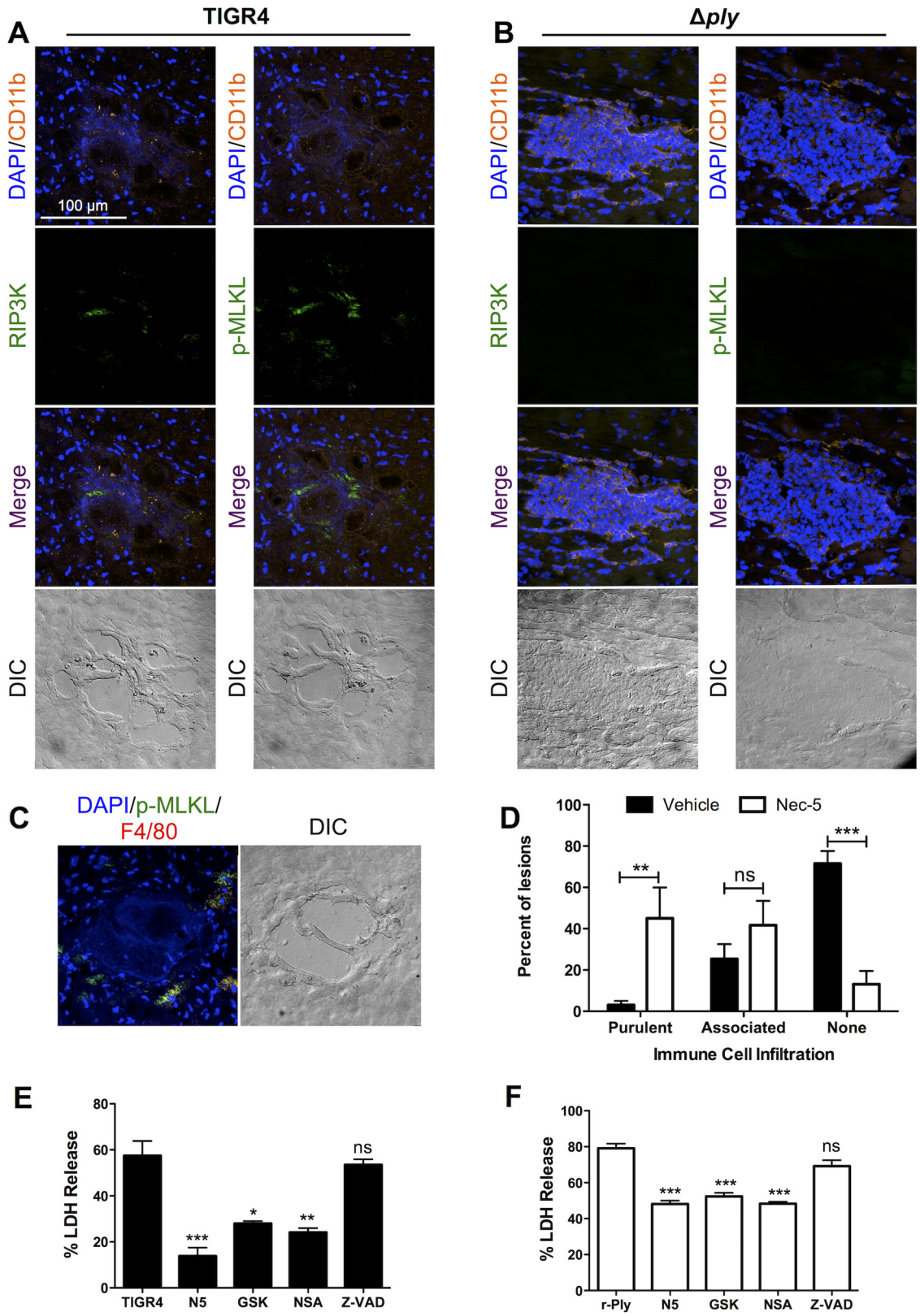

FIG 7 Infiltrated immune cells die due partially to necroptosis. (A to C) Representative IFM images of stained serial frozen sections from mice challenged with TIGR4 (A) and TIGR4 Δ*ply* (B) costained for DAPI, CD11b, and either p-MLKL or RIP3 kinase or mice challenged with TIGR4 costained for DAPI, p-MLKL, and F4/80 (C). Magnification, ×40 with a zoom factor of 1.0. (D) Percentage of microlesions from each mouse that either were fully purulent, contained peripherally associated immune cells, or were completely devoid of immune cells (as determined at a ×25 magnification) following infection of mice with TIGR4 and treatment of mice with necrostatin-5 (Nec-5) or the vehicle as a control. THP-1 macrophages were pretreated with necrostatin-5 (N5), GSK'872 (GSK), necrosulfonamide (NSA), or Z-VAD-FMK (Z-VAD) and challenged with either TIGR4 (E) or recombinant pneumolysin (r-Ply) (F). For panels E and F, cell death was measured by determination of the amount of lactate dehydrogenase (LDH) in the supernatants, *, $P \leq 0.05$; **, $P \leq 0.01$; ***, $P \leq 0.001$; ns, not significant.

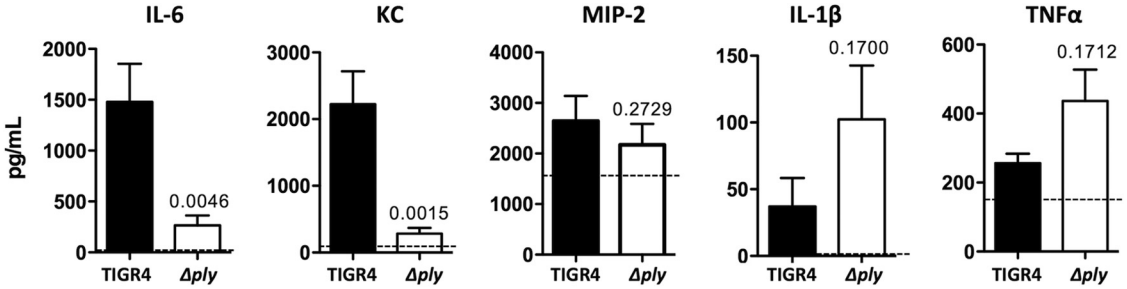

FIG 8 Cytokines and chemokines are present in cardiac tissue during IPD. The concentrations of the indicated cytokines and chemokines in homogenates of heart tissue obtained at 42 hpi from either TIGR4- or TIGR4 Δ*ply*-infected mice were determined by ELISAs. *P* values determined by a two-tailed Student's *t* test are indicated. Dashed lines, median level observed for uninfected hearts. Data are for >6 mice for all cohorts.

of the production of the other cytokines and chemokines measured (i.e., IL-1β, TNF-α, and MIP-2).

Following severe ischemia, cardiomyocytes die as a result of necroptosis. Luedde et al. have demonstrated that this contributes to the adverse cardiac remodeling that can occur following an infarct (22). Of note, mice deficient in RIP3 showed a better ejection fraction and less hypertrophy in the 30 days after experimental infarction by coronary artery ligation (22). In the study described in our first report that described cardiac microlesions, we observed that cardiac microlesions became foci of extensive collagen remodeling in antimicrobial-rescued mice that had been infected with TIGR4 (11). As such, macrophage necroptosis and perhaps even cardiomyocyte necroptosis may contribute to the remodeling that is observed following invasive pneumococcal disease. Whether the neutralization of pneumolysin or the blocking of necroptosis during infection is beneficial remains unknown. Microlesions continued to form and grew in size both in mice infected with TIGR4 Δ*ply* and in TIGR4-infected necrostatin-5-treated mice, yet for mice infected with D39, these treatments would presumably confer cardiac protection, since pneumolysin is requisite for cardiac damage. Determination of whether cardiac scarring occurs and whether changes in the extent of remodeling occur in mice treated with antibodies against pneumolysin or necrostatin-5 is important to elucidate the potential of these interventions to prevent adverse cardiac events during convalescence.

In summary, this report provides direct evidence that pneumococci invade the myocardium during IPD. Depending on the infecting strain, this can result in a distinct pathology. Here, in mice infected with the laboratory strains TIGR4 and D39, we observed highly discrete cardiac microlesions filled with pneumococci or areas where bacteria were not readily visible until they were detected by IFM, but cardiac damage in the form of hydropic degeneration and immune cell infiltration, respectively, occurred. We demonstrate that the requirement for pneumolysin in cardiac damage is strain dependent but that pneumolysin modulates the host response. It does this both by killing infiltrated macrophages via necroptosis and by potentiating the cytokine and chemokine response during infection. These findings support the notion that cardiac invasion is a means by which the pneumococci directly deliver cardiotoxic products to cardiomyocytes and these products contribute to the development of adverse cardiac events during or after CAP.

ACKNOWLEDGMENTS

We thank Alexis Herrera for her work sectioning the frozen hearts and Monica Alarcon and Barbara Hunter for their efforts in preparing the tissue sections for electron microscopy.

FUNDING INFORMATION

This work, including the efforts of Carlos J Orihuela, was funded by HHS | National Institutes of Health (NIH) (R01AI114800). This work, including the efforts of Carlos J Orihuela, was funded by American Heart Association (AHA) (13IRG14560023).

The funders had no role in study design, data collection and interpretation, or the decision to submit the work for publication.

REFERENCES

1. **Kochanek KD, Xu J, Murphy SL, Minino AM, Kung HC.** 2011. Deaths: preliminary data for 2009. Natl Vital Stat Rep **59:**1–51.
2. **Lozano R, Naghavi M, Foreman K, Lim S, Shibuya K, Aboyans V, Abraham J, Adair T, Aggarwal R, Ahn SY, Alvarado M, Anderson HR, Anderson LM, Andrews KG, Atkinson C, Baddour LM, Barker-Collo S, Bartels DH, Bell ML, Benjamin EJ, Bennett D, Bhalla K, Bikbov B, Bin Abdulhak A, Birbeck G, Blyth F, Bolliger I, Boufous S, Bucello C, Burch M, Burney P, Carapetis J, Chen H, Chou D, Chugh SS, Coffeng LE, Colan SD, Colquhoun S, Colson KE, Condon J, Connor MD, Cooper LT, Corriere M, Cortinovis M, de Vaccaro KC, Couser W, Cowie BC, Criqui MH, Cross M, Dabhadkar KC, et al.** 2012. Global and regional mortality from 235 causes of death for 20 age groups in 1990 and 2010: a systematic analysis for the Global Burden of Disease Study 2010. Lancet **380:**2095–2128. http://dx.doi.org/10.1016/S0140-6736(12)61728-0.
3. **Wunderink RG, Waterer GW.** 2014. Community-acquired pneumonia. N Engl J Med **370:**1863. http://dx.doi.org/10.1056/NEJMc1402692.
4. **Corrales-Medina VF, Musher DM, Wells GA, Chirinos JA, Chen L, Fine MJ.** 2012. Cardiac complications in patients with community-acquired pneumonia: incidence, timing, risk factors, and association with short-term mortality. Circulation **125:**773–781. http://dx.doi.org/10.1161/CIRCULATIONAHA.111.040766.
5. **Corrales-Medina VF, Serpa J, Rueda AM, Giordano TP, Bozkurt B, Madjid M, Tweardy D, Musher DM.** 2009. Acute bacterial pneumonia is associated with the occurrence of acute coronary syndromes. Medicine (Baltimore, MD) **88:**154–159. http://dx.doi.org/10.1097/MD.0b013e3181a692f0.
6. **Corrales-Medina VF, Taljaard M, Yende S, Kronmal R, Dwivedi G, Newman AB, Elkind MS, Lyles MF, Chirinos JA.** 2015. Intermediate and long-term risk of new-onset heart failure after hospitalization for pneumonia in elderly adults. Am Heart J **170:**306–312. http://dx.doi.org/10.1016/j.ahj.2015.04.028.
7. **Perry TW, Pugh MJ, Waterer GW, Nakashima B, Orihuela CJ, Copeland LA, Restrepo MI, Anzueto A, Mortensen EM.** 2011. Incidence of cardiovascular events after hospital admission for pneumonia. Am J Med **124:**244–251. http://dx.doi.org/10.1016/j.amjmed.2010.11.014.
8. **Musher DM, Rueda AM, Kaka AS, Mapara SM.** 2007. The association between pneumococcal pneumonia and acute cardiac events. Clin Infect Dis **45:**158–165. http://dx.doi.org/10.1086/518849.

9. **Naucler P, Darenberg J, Morfeldt E, Ortqvist A, Henriques Normark B.** 2013. Contribution of host, bacterial factors and antibiotic treatment to mortality in adult patients with bacteraemic pneumococcal pneumonia. Thorax **68:**571–579. http://dx.doi.org/10.1136/thoraxjnl-2012-203106.
10. **Brown AO, Millett ER, Quint JK, Orihuela CJ.** 2015. Cardiotoxicity during invasive pneumococcal disease. Am J Respir Crit Care Med **191:** 739–745. http://dx.doi.org/10.1164/rccm.201411-1951PP.
11. **Brown AO, Mann B, Gao G, Hankins JS, Humann J, Giardina J, Faverio P, Restrepo MI, Halade GV, Mortensen EM, Lindsey ML, Hanes M, Happel KI, Nelson S, Bagby GJ, Lorent JA, Cardinal P, Granados R, Esteban A, LeSaux CJ, Tuomanen EI, Orihuela CJ.** 2014. Streptococcus pneumoniae translocates into the myocardium and forms unique microlesions that disrupt cardiac function. PLoS Pathog **10:**e1004383. http://dx.doi.org/10.1371/journal.ppat.1004383.
12. **Jedrzejas MJ.** 2001. Pneumococcal virulence factors: structure and function. Microbiol Mol Biol Rev **65:**187–207. http://dx.doi.org/10.1128/MMBR.65.2.187-207.2001.
13. **Fillon S, Soulis K, Rajasekaran S, Benedict-Hamilton H, Radin JN, Orihuela CJ, El Kasmi KC, Murti G, Kaushal D, Gaber MW, Weber JR, Murray PJ, Tuomanen EI.** 2006. Platelet-activating factor receptor and innate immunity: uptake of gram-positive bacterial cell wall into host cells and cell-specific pathophysiology. J Immunol **177:**6182–6191. http://dx.doi.org/10.4049/jimmunol.177.9.6182.
14. **Alhamdi Y, Neill DR, Abrams ST, Malak HA, Yahya R, Barrett-Jolley R, Wang G, Kadioglu A, Toh CH.** 2015. Circulating pneumolysin is a potent inducer of cardiac injury during pneumococcal infection. PLoS Pathog **11:**e1004836. http://dx.doi.org/10.1371/journal.ppat.1004836.
15. **Tettelin H, Nelson KE, Paulsen IT, Eisen JA, Read TD, Peterson S, Heidelberg J, DeBoy RT, Haft DH, Dodson RJ, Durkin AS, Gwinn M, Kolonay JF, Nelson WC, Peterson JD, Umayam LA, White O, Salzberg SL, Lewis MR, Radune D, Holtzapple E, Khouri H, Wolf AM, Utterback TR, Hansen CL, McDonald LA, Feldblyum TV, Angiuoli S, Dickinson T, Hickey EK, Holt IE, Loftus BJ, Yang F, Smith HO, Venter JC, Dougherty BA, Morrison DA, Hollingshead SK, Fraser CM.** 2001. Complete genome sequence of a virulent isolate of Streptococcus pneumoniae. Science **293:**498–506. http://dx.doi.org/10.1126/science.1061217.
16. **Lanie JA, Ng WL, Kazmierczak KM, Andrzejewski TM, Davidsen TM, Wayne KJ, Tettelin H, Glass JI, Winkler ME.** 2007. Genome sequence of Avery's virulent serotype 2 strain D39 of Streptococcus pneumoniae and comparison with that of unencapsulated laboratory strain R6. J Bacteriol **189:**38–51. http://dx.doi.org/10.1128/JB.01148-06.
17. **Spellerberg B, Cundell DR, Sandros J, Pearce BJ, Idanpaan-Heikkila I, Rosenow C, Masure HR.** 1996. Pyruvate oxidase, as a determinant of virulence in Streptococcus pneumoniae. Mol Microbiol **19:**803–813. http://dx.doi.org/10.1046/j.1365-2958.1996.425954.x.
18. **Pasparakis M, Vandenabeele P.** 2015. Necroptosis and its role in inflammation. Nature **517:**311–320. http://dx.doi.org/10.1038/nature14191.
19. **Dannappel M, Vlantis K, Kumari S, Polykratis A, Kim C, Wachsmuth L, Eftychi C, Lin J, Corona T, Hermance N, Zelic M, Kirsch P, Basic M, Bleich A, Kelliher M, Pasparakis M.** 2014. RIPK1 maintains epithelial homeostasis by inhibiting apoptosis and necroptosis. Nature **513:**90–94. http://dx.doi.org/10.1038/nature13608.
20. **Vandenabeele P, Galluzzi L, Vanden Berghe T, Kroemer G.** 2010. Molecular mechanisms of necroptosis: an ordered cellular explosion. Nat Rev Mol Cell Biol **11:**700–714. http://dx.doi.org/10.1038/nrm2970.
21. **Gonzalez-Juarbe N, Mares CA, Hinojosa CA, Medina JL, Cantwell A, Dube PH, Orihuela CJ, Bergman MA.** 2015. Requirement for Serratia marcescens cytolysin in a murine model of hemorrhagic pneumonia. Infect Immun **83:**614–624. http://dx.doi.org/10.1128/IAI.01822-14.
22. **Luedde M, Lutz M, Carter N, Sosna J, Jacoby C, Vucur M, Gautheron J, Roderburg C, Borg N, Reisinger F, Hippe HJ, Linkermann A, Wolf MJ, Rose-John S, Lullmann-Rauch R, Adam D, Flogel U, Heikenwalder M, Luedde T, Frey N.** 2014. RIP3, a kinase promoting necroptotic cell death, mediates adverse remodelling after myocardial infarction. Cardiovasc Res **103:**206–216. http://dx.doi.org/10.1093/cvr/cvu146.
23. **National Research Council.** 2011. Guide for the care and use of laboratory animals, 8th ed. National Academies Press, Washington, DC.
24. **Lizcano A, Chin T, Sauer K, Tuomanen EI, Orihuela CJ.** 2010. Early biofilm formation on microtiter plates is not correlated with the invasive disease potential of Streptococcus pneumoniae. Microb Pathog **48:**124–130. http://dx.doi.org/10.1016/j.micpath.2010.01.002.
25. **Shivshankar P, Sanchez C, Rose LF, Orihuela CJ.** 2009. The Streptococcus pneumoniae adhesin PsrP binds to Keratin 10 on lung cells. Mol Microbiol **73:**663–679. http://dx.doi.org/10.1111/j.1365-2958.2009.06796.x.
26. **McDaniel LS, Yother J, Vijayakumar M, McGarry L, Guild WR, Briles DE.** 1987. Use of insertional inactivation to facilitate studies of biological properties of pneumococcal surface protein A (PspA). J Exp Med **165:** 381–394. http://dx.doi.org/10.1084/jem.165.2.381.
27. **Tu AH, Fulgham RL, McCrory MA, Briles DE, Szalai AJ.** 1999. Pneumococcal surface protein A inhibits complement activation by Streptococcus pneumoniae. Infect Immun **67:**4720–4724.
28. **Austyn JM, Gordon S.** 1981. F4/80, a monoclonal antibody directed specifically against the mouse macrophage. Eur J Immunol **11:**805–815. http://dx.doi.org/10.1002/eji.1830111013.
29. **Gabrilovich DI, Nagaraj S.** 2009. Myeloid-derived suppressor cells as regulators of the immune system. Nat Rev Immunol **9:**162–174. http://dx.doi.org/10.1038/nri2506.
30. **Gonzalez-Juarbe N, Gilley RP, Hinojosa CA, Bradley KM, Kamei A, Gao G, Dube PH, Bergman MA, Orihuela CJ.** 2015. Pore-forming toxins induce macrophage necroptosis during acute bacterial pneumonia. PLoS Pathog **11:**e1005337. http://dx.doi.org/10.1371/journal.ppat.1005337.
31. **Kitur K, Parker D, Nieto P, Ahn DS, Cohen TS, Chung S, Wachtel S, Bueno S, Prince A.** 2015. Toxin-induced necroptosis is a major mechanism of Staphylococcus aureus lung damage. PLoS Pathog **11:**e1004820. http://dx.doi.org/10.1371/journal.ppat.1004820.
32. **Sun L, Wang H, Wang Z, He S, Chen S, Liao D, Wang L, Yan J, Liu W, Lei X, Wang X.** 2012. Mixed lineage kinase domain-like protein mediates necrosis signaling downstream of RIP3 kinase. Cell **148:**213–227. http://dx.doi.org/10.1016/j.cell.2011.11.031.
33. **Wang Z, Jiang H, Chen S, Du F, Wang X.** 2012. The mitochondrial phosphatase PGAM5 functions at the convergence point of multiple necrotic death pathways. Cell **148:**228–243. http://dx.doi.org/10.1016/j.cell.2011.11.030.
34. **Zhao J, Jitkaew S, Cai Z, Choksi S, Li Q, Luo J, Liu ZG.** 2012. Mixed lineage kinase domain-like is a key receptor interacting protein 3 downstream component of TNF-induced necrosis. Proc Natl Acad Sci U S A **109:**5322–5327. http://dx.doi.org/10.1073/pnas.1200012109.
35. **Corrales-Medina VF, Suh KN, Rose G, Chirinos JA, Doucette S, Cameron DW, Fergusson DA.** 2011. Cardiac complications in patients with community-acquired pneumonia: a systematic review and meta-analysis of observational studies. PLoS Med **8:**e1001048. http://dx.doi.org/10.1371/journal.pmed.1001048.
36. **Corrales-Medina VF, Musher DM, Shachkina S, Chirinos JA.** 2013. Acute pneumonia and the cardiovascular system. Lancet **381:**496–505. http://dx.doi.org/10.1016/S0140-6736(12)61266-5.
37. **Mortensen EM, Halm EA, Pugh MJ, Copeland LA, Metersky M, Fine MJ, Johnson CS, Alvarez CA, Frei CR, Good C, Restrepo MI, Downs JR, Anzueto A.** 2014. Association of azithromycin with mortality and cardiovascular events among older patients hospitalized with pneumonia. JAMA **311:**2199–2208. http://dx.doi.org/10.1001/jama.2014.4304.
38. **Boyd JH, Mathur S, Wang Y, Bateman RM, Walley KR.** 2006. Toll-like receptor stimulation in cardiomyocytes decreases contractility and initiates an NF-kappaB dependent inflammatory response. Cardiovasc Res **72:**384–393. http://dx.doi.org/10.1016/j.cardiores.2006.09.011.
39. Reference deleted.
40. **Cain BS, Meldrum DR, Dinarello CA, Meng X, Joo KS, Banerjee A, Harken AH.** 1999. Tumor necrosis factor-alpha and interleukin-1beta synergistically depress human myocardial function. Crit Care Med **27:** 1309–1318. http://dx.doi.org/10.1097/00003246-199907000-00018.
41. **Wade KR, Hotze EM, Briles DE, Tweten RK.** 2014. Mouse, but not human, ApoB-100 lipoprotein cholesterol is a potent innate inhibitor of Streptococcus pneumoniae pneumolysin. PLoS Pathog **10:**e1004353. http://dx.doi.org/10.1371/journal.ppat.1004353.
42. **Bek-Thomsen M, Poulsen K, Kilian M.** 2012. Occurrence and evolution of the paralogous zinc metalloproteases IgA1 protease, ZmpB, ZmpC, and ZmpD in Streptococcus pneumoniae and related commensal species. mBio **3:**e00303-12. http://dx.doi.org/10.1128/mBio.00303-12.
43. **Mosser EM, Rest RF.** 2006. The Bacillus anthracis cholesterol-dependent cytolysin, anthrolysin O, kills human neutrophils, monocytes and macrophages. BMC Microbiol **6:**56. http://dx.doi.org/10.1186/1471-2180-6-56.

44. **Urban CF, Lourido S, Zychlinsky A.** 2006. How do microbes evade neutrophil killing? Cell Microbiol **8:**1687–1696. http://dx.doi.org/10.1111/j.1462-5822.2006.00792.x.
45. **Duprez L, Takahashi N, Van Hauwermeiren F, Vandendriessche B, Goossens V, Vanden Berghe T, Declercq W, Libert C, Cauwels A, Vandenabeele P.** 2011. RIP kinase-dependent necrosis drives lethal systemic inflammatory response syndrome. Immunity **35:**908–918. http://dx.doi.org/10.1016/j.immuni.2011.09.020.
46. **Boyd AR, Shivshankar P, Jiang S, Berton MT, Orihuela CJ.** 2012. Age-related defects in TLR2 signaling diminish the cytokine response by alveolar macrophages during murine pneumococcal pneumonia. Exp Gerontol **47:**507–518. http://dx.doi.org/10.1016/j.exger.2012.04.004.